Supplementary Materials belonging to

Solution conformation of the 70 kDa *E.coli* Hsp70 complexed with ADP and substrate.

Eric B. Bertelsen[1] , Lyra Chang[2], Jason E. Gestwicki[2] and Erik R. P. Zuiderweg[1]*

Departments of Biological Chemistry[1] and Pathology[2], The University of Michigan, Ann Arbor, MI 48109, USA.

(1) **Dynamics**	**(Figures S1-S3, Table S1)**	**page 2**
(2) Activity assay	**(Figures S4 and S5)**	**page 6**
(3) Details of RDC calculations	**(Tables S2-S8)**	**page 8**

(1) **Dynamics.**

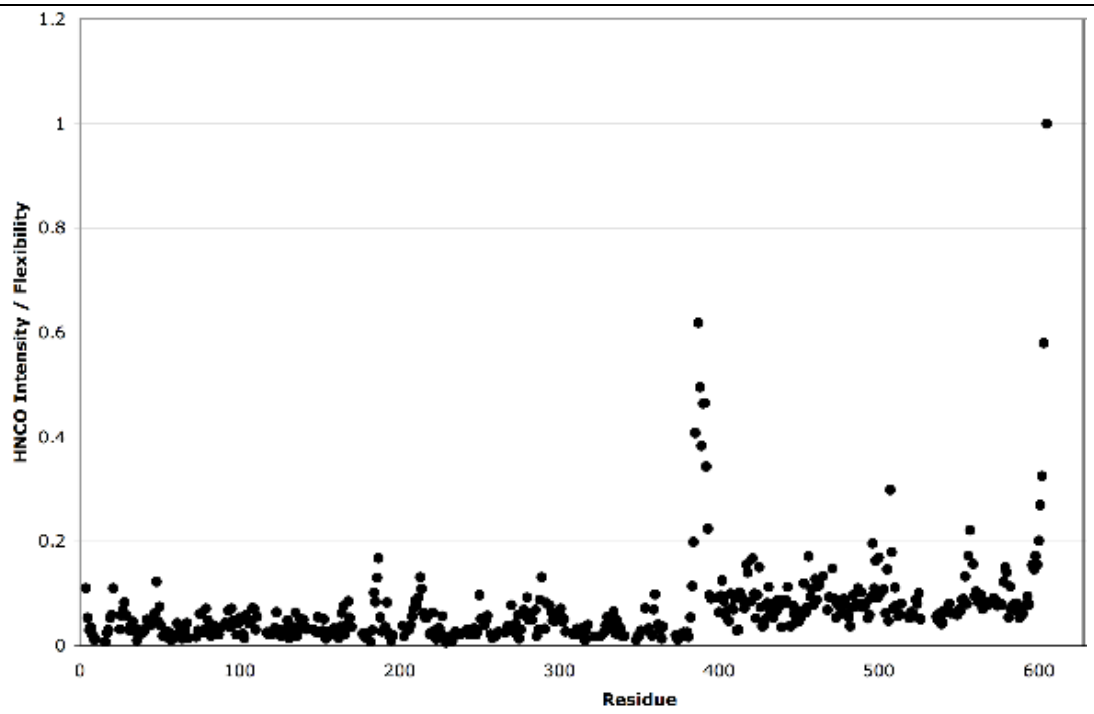

Figure S1. Domain-level dynamics.
Normalized HNCO-TROSY peak intensities are plotted as a function of residue number for DnaK 1-605 in the presence of ADP, inorganic phosphate, and peptide NRLLLTG. Residues 1-385 are in the NBD with an average intensity of 0.040±0.025 arbitrary units; residues 385-395 are in the linker; residues 396-500 are in BETA with an average intensity of 0.086±0.034 arbitrary units ; residues 501-603 are in the LID with an average intensity of 0.090 ±0.037 arbitrary units.

The major determinant of the peak height in the HNCO shown in Figure S1 is the overall rotational correlation time and local mobility in the sub-nano second time domain. In HNCO, faster local motions allow for less relaxation during the course of the delays in the pulse sequence, yielding larger 3D cross peaks. All delays, whether the coherence resides on the amide proton, the amide nitrogen, or the carbonyl carbon, are affected. As such, peak intensities in the HNCO experiment are perhaps indicators of more “isotropic” dynamics as compared to the classical ^{15}N relaxation measurements that report on the reorientational dynamics of the NH vectors only.

^{15}N R_1 and R_2 TROSY experiments (1) were used to obtain estimates of the correlation times of the SBD and NBD in the full construct. The values obtained are listed under the header τ_C^{EXP} in Table S1.

Table S1. Experimental and calculated rotational correlation times

domain	X[a]	Y[a]	Z[a]	$\tau_{isolated}^{domain}$ [c]	τ_{local}^{domain} [d]	$\tau_{local}^{domain} / \tau_{isolated}^{computed}$	τ_C^{EXP} [e]
	Å	Å	Å	ns	ns		ns
SBD	22	43	62	8.03	39	4.9	22
NBD	53	52	63	17.77	75	4.2	30
Full construct[b]	53	52	128	50.63			

[a] diameters of the domains from the crystal structures
[b] diameters of the hybrid structure described in this report
[c] average correlation times computed from the coordinates using the Woessner formalism (2) with an axial symmetry approximation, at 27 ^{0}C.
[d] obtained from equation (1).
[e] Measured at 27 ^{0}C.

The values in Table S1 were used to obtain an estimate of the amplitude of the motion of the two domains with respect to each other as follows.
Under the assumption of decoupling between overall and domain motion, one may write

$$\frac{1}{\tau_{Eff}^{domain}} = \frac{1}{\tau_c^{overall}} + \frac{1}{\tau_{local}^{domain}} \qquad [1]$$

τ_{Eff}^{domain} should correspond to the measured quantity τ_C^{EXP} ; the other two quantities are unknown. We compute $\tau_c^{overall}$ from the average structure, using the Woessner formalism (2) (column $\tau_{isolated}^{computed}$ in Table S1). This allows us to estimate τ_{local}^{domain} from Equation (1). τ_{local}^{domain} should equate the local correlation times for the domains in the full construct, when their motions are restricted due to the linker.
As a next step, we compare the values of τ_{local}^{domain} with the calculated correlation times for the domains, $\tau_{isolated}^{domain}$, i.e. the correlation times when these domains would move freely in solution, or completely loosely tethered (as beads on a flexible string).
Taking the ratio of the two yields the immobilization factor due to the tethering. This factor can be used to estimate a limit on the angle of the restricted motional cone of the domains using a reformatted version equation A4 of (3):

$$\frac{\tau_{local}^{domain}}{\tau_{isolated}^{domain}} = \frac{6}{1 - S_{cone}^2}\left[A - B\right] \qquad [2]$$

where

$$A = \frac{(1-c)}{24}\left(6 + 8c - c^2 - 12c^3 - 7c^4\right)$$

$$B = \frac{c^2(1+c)^2}{2(c-1)}\left\{{}^{10}\log\left[(1+c)/2\right] + (1-c)/2\right\} \qquad [3]$$

with $c = \cos\theta$, where θ is one-half of the opening angle of the cone that describes the limit of the motion, and where

$$S^2_{cone} = \left\{\frac{c(1+c)}{2}\right\}^2 \qquad [4]$$

For $\tau^{domain}_{local} / \tau^{computed}_{isolated}$ =4.9 and 4.2, we find θ =33 and 35 degrees, respectively. We take the average of 34 degrees as describing the opening cone angle for the SBD with respect to the NBD and vice versa.

This cone angle yields a squared order parameter of 0.57, relevant for relaxation, and a order parameter of 0.75, relevant for RDC measurements.

Dynamical averaging.
Four models for DnaK were constructed, in which the SBD/LID domains were rotated away by 35 degrees from the length axis of the conformation shown in Figure 1 of the main text. These structures may represent the extend of dynamical averaging as computed above (see Fig S2). Next, we predicted the RDC's for these four models, and averaged them. Subsequently, we computed a structure compatible with these averaged RDC's. The resulting conformation, shown in figure S3, together with the structure obtained from the experimental RDC's. The overall orientation is retained, showing that dynamical averaging of RDC's can still lead to an "existable" structure compatible with our data.

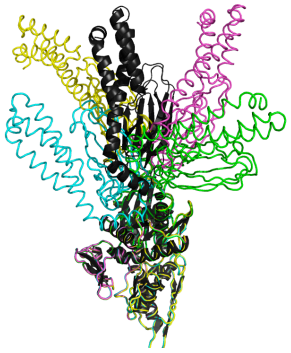

Fig S2. Test conformations of DnaK, with the SBD rotated away at the linker (colors) with the structure of Fig 1 in black.

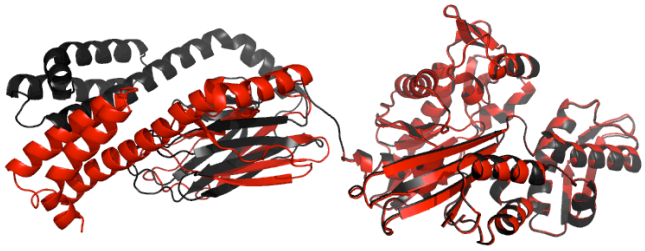

Fig S3. The structure of DnaK of Fig 1 in black, with a structure computed from the averaged RDC's of the four colored structures in Fig S2, in red.

(2) Activity assay

The mutant *E. Coli* DnaK(1-605) V210C was prepared using Stratagene mutagenesis kit. The activity of this protein was measured and compared to that of wt-DnaK *E. coli* (1-638) with an ATP hydrolysis assay using malachite-green as a detector of released inorganic phosphate (4). Total DnaK: 14 picomoles; total DnaJ, 25 picomoles. Total ATP: 25 picomoles. ATP concentration: 1 mM. Figure S4 shows that the ATP hydrolysis activity of DnaK(1-605) V210C is indistinguishable from that of wt-DnaK (1-638). Figure S4 shows that DnaJ (*E. coli*) stimulates the ATP hydrolysis activity of DnaK(1-605) V210C equally well as wt DnaK.

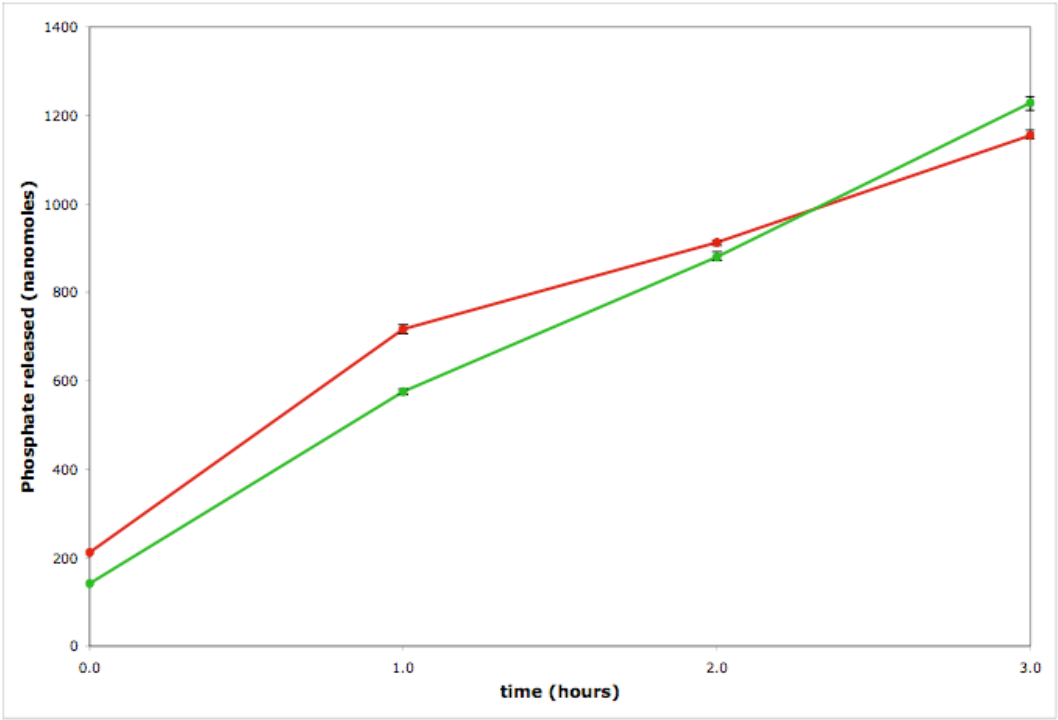

Figure S4. ATP hydrolysis assay of wt-DnaK *E. coli* (green) and DnaK(1-605) V210C (red). Each time point was taken in triplicate. Total DnaK: 14 picomoles, total ATP: 25 picomoles

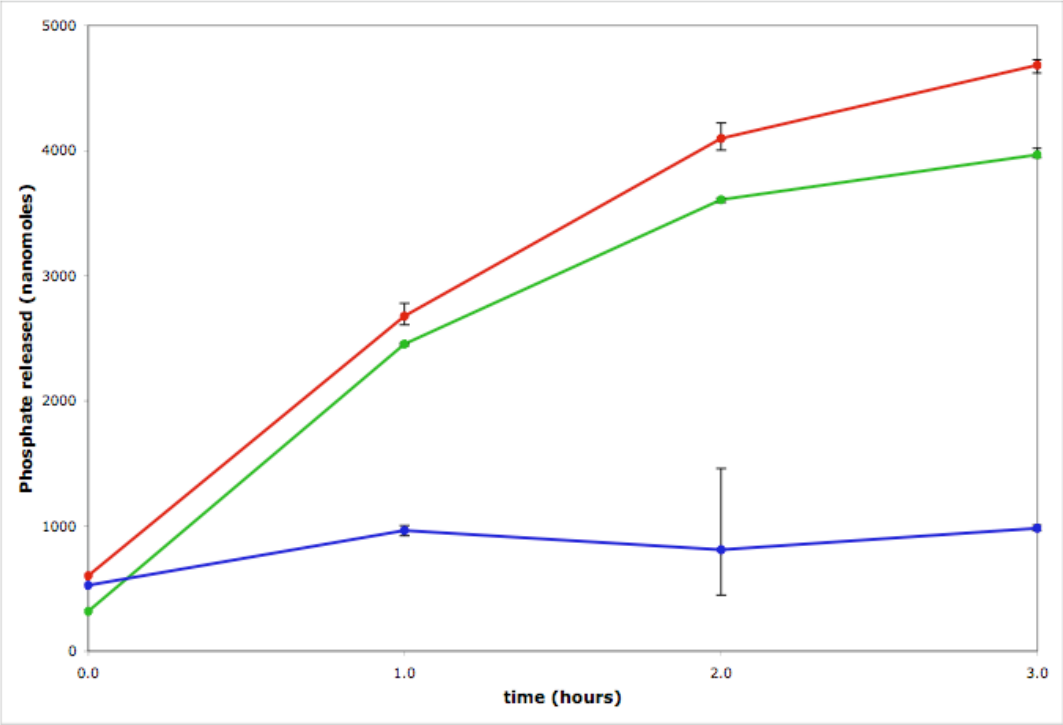

Figure S5. ATP hydrolysis assay of wt-DnaK *E. coli* (green) and DnaK(1-605) V210C (red) in the presence of 2-fold excess of DnaJ E.coli. The ATP hydrolysis of DnaJ alone is shown in blue. Each time point was taken in triplicate. Total DnaK: 14 picomoles; total DnaJ, 25 picomoles; total ATP: 25 picomoles.

(3) Details of RDC calculations

Supplementary Table S2. Sub-domain-specific RDC calculation statistics

	ndip[k]	D_A [c]	D_R/D_A	Θ_z [e]	Φ_x [f]	RMSD [g]	Q [h]	S_{zz}	S_{yy}	S_{xx}	GDO [i]	η [j]
NBD IA												
Best_fit[a]	32	-14.25	0.30	**-2.94**	10.70	4.87	0.34	-1.17E-03	8.51E-04	3.19E-04	1.21E-03	0.45
Rmsd Of self-validation[b]		1.38	0.12	**6.26**	14.94	0.56	0.05	1.13E-04	9.42E-05	1.34E-04	1.04E-04	0.18
NBD IB												
Best_fit[a]	38	-10.82	0.30	**-1.55**	-4.80	6.41	0.53	-8.89E-04	6.41E-04	2.48E-04	9.17E-04	0.44
Rmsd Of self-validation[b]		1.64	0.13	**4.88**	11.03	1.28	0.10	1.35E-04	1.11E-04	9.76E-05	1.35E-04	0.19
NBD IIA												
Best_fit[a]	35	-10.78	0.28	**-2.57**	-9.90	4.94	0.44	-8.85E-04	6.27E-04	2.59E-04	9.10E-04	0.42
Rmsd Of self-validation[b]		1.27	0.10	3.53	15.65	0.55	0.06	1.04E-04	6.35E-05	8.53E-05	9.69E-05	0.15
NBD-IIB												
Best_fit[a]	26	-12.10	0.22	**19.64**	24.50	3.74	0.32	-9.94E-04	6.64E-04	3.30E-04	1.01E-03	0.34
Rmsd Of self-validation[b]		1.45	0.16	**13.25**	13.88	0.77	0.07	1.19E-04	1.08E-04	1.46E-04	1.11E-04	0.24

Supplementary Table 2, continued

	ndip[k]	D_A [c]	D_R/D_A	Θ_z [e]	Φ_x [f]	RMSD [g]	Q [h]	S_{zz}	S_{yy}	S_{xx}	GDO [i]	η [j]
SBD-BETA												
Best_fit[a]	58	-14.69	0.30	-6.46	1.98	2.44	0.17	-1.21E-03	8.75E-04	3.31E-04	1.25E-03	0.45
Rmsd Of self-validation[b]		0.61	0.03	2.22	4.35	0.44	0.03	5.01E-05	2.09E-05	4.34E-05	4.46E-05	0.05
SBD-LID												
Best_fit[a]	21	-12.53	0.29	-5.40	-6.69	2.70	0.21	-1.03E-03	7.37E-04	2.92E-04	1.06E-03	0.43
Rmsd Of self-validation[b]		1.21	0.09	5.27	10.59	0.73	0.06	9.95E-05	1.07E-04	7.91E-05	1.09E-04	0.14

a) Best fits were computed using a grid-search program optimizing DA, DR/DA, and the three tensor orientation angles.
b) Thirty fits were computed for NBD and SBD each using on average 50% of the RDC data, randomly picked.
c) $D_A = \left(S_{ZZ} - \left(S_{YY} + S_{XX}\right)/2\right) * D_{MAX}$ where D_{MAX} is the full dipolar coupling (22 KHz)
d) $D_R = \left(S_{XX} - S_{YY}\right) * D_{MAX}$
e) The angle of the Szz direction in the self-validation with the Szz direction in the PAS as defined from the best fit
f) The angle of the Sxx direction in the self-validation with the Sxx direction in the PAS as defined from the best fit

g) RMSD or RDC fit

h) $$Q = \frac{RMSD}{\sqrt{\frac{\sum_{i=1}^{N_{RDC}} \left(RDC(i)_{\exp}\right)^2}{N_{RDC}}}}$$

i) $$GDO = \sqrt{\frac{2}{3}\left(S_{zz}^2 + S_{yy}^2 + S_{xx}^2\right)}$$

j) $$\eta = \left(S_{xx} - S_{yy}\right)/S_{zz}$$

k) NDIP= number of dipoles.

Supplementary Table 3 [a]								
	DA	DR/DA	GDO	η	Θ(z)	Φ(x)	RMSD	Q
	(Hz)				(degree)	(degree)		
Reference[b]	-13.02	0.30	1.11E-03	0.45	-0.04	-0.04	0.04	0.00
Str error[c]								
5°	-12.85±0.16[e]	0.29±0.02	1.09E-03±1.19E-05	0.43±0.03	-1.08±0.68	-1.66±1.74	2.14±0.27	0.17±0.02
10°	-12.61±0.51	0.24±0.04	1.06E-03±3.96E-05	0.36±0.05	-2.82±1.12	-5.02±3.43	3.84±0.48	0.31±0.04
15°	-11.58±0.75	0.20±0.09	9.67E-04±5.49E-05	0.29±0.14	-1.82±3.64	-10.79±13.03	5.67±0.65	0.47±0.05
20°	-10.88±0.84	0.12±0.11	9.01E-04±6.57E-05	0.18±0.17	2.94±5.19	2.84±36.50	7.11±0.45	0.59±0.04
RDC error[d]								
2 Hz	-12.97±0.15	0.29±0.01	1.10E-03±1.39E-05	0.44±0.02	-0.51±0.38	-0.71±1.45	1.93±0.14	0.16±0.01
4 Hz	-13.14±0.59	0.31±0.04	1.12E-03±4.35E-05	0.47±0.06	-1.03±0.90	-1.38±3.79	3.82±0.20	0.29±0.02
6 Hz	-13.07±0.74	0.33±0.04	1.12E-03±6.08E-05	0.49±0.05	-1.58±1.02	-1.46±4.95	5.68±0.50	0.41±0.04

a) Calculations of the effects of structural and RDC measurement uncertainties on alignment parameters.

The column entries are defined in the legend to Supplementary table 2.

b) calculation for 108 experimental RDC's for domains IA+IB+IIA

c) Each of the three Euler angles of the individual NH vectors in the structure were randomly varied in a range of ± the indicated angles. Ten of such calculations were made for each of the indicated error ranges.

d) The experimental RDC's were randomly varied in a range of ± the indicated frequencies. Ten of such calculations were made for each of the indicated error ranges.

e) the number here, and in every other table entry, lists the RMSD for the ten calculations.

Supplementary Table 4

Computations of the theoretical alignment tensor orientation using the program Pales.

	z[a]	y[a]	x[a]	$\alpha+\beta+\gamma$[b]	η[c]
Experimental NBD in 1-605	NA	NA	NA	**0**	**0.46**
Experimental SBD in 1-605	NA	NA	NA	**0**	**0.47**
Pales NBD alone	NA	NA	NA	**28.58**	**0.63 (0.45/0.41[d])**
Pales SBD alone	NA	NA	NA	**9.26**	**0.88**
Pales 1-605 model 1	-70	-15	-5	6.13	0.52
Pales 1-605 model 2	-70	-15	0	3	0.51
Pales 1-605 model 3	-70	-15	5	5.51	0.49
Pales 1-605 model 4	-70	-10	-5	6.32	0.48
Pales 1-605 model 5	**-70**	**-10**	**0**	**2.47**	**0.48**
Pales 1-605 model 6	-70	-10	5	5.5	0.46
Pales 1-605 model 7	-70	-5	-5	9.3	0.43
Pales 1-605 model 8	-70	-5	0	5.83	0.43
Pales 1-605 model 9	-70	-5	5	7.55	0.40
Pales 1-605 model 10	-65	-15	-5	6.72	0.54
Pales 1-605 model 11	-65	-15	0	3.57	0.54
Pales 1-605 model 12	-65	-15	5	5.55	0.51
Pales 1-605 model 13	-65	-10	-5	6.42	0.50
Pales 1-605 model 14	**-65**	**-10**	**0**	**2.89**	**0.50**
Pales 1-605 model 15	-65	-10	5	5.13	0.47
Pales 1-605 model 16	-65	-5	-5	9.16	0.45
Pales 1-605 model 17	-65	-5	0	6.48	0.45
Pales 1-605 model 18	-65	-5	5	7.11	0.42
Pales 1-605 model 19	-60	-15	-5	7.24	0.55
Pales 1-605 model 20	-60	-15	0	4.15	0.56
Pales 1-605 model 21	-60	-15	5	5.36	0.54
Pales 1-605 model 22	-60	-10	-5	6.41	0.52
Pales 1-605 model 23	**-60**	**-10**	**0**	**3.22**	**0.52**
Pales 1-605 model 24	-60	-10	5	4.96	0.50
Pales 1-605 model 25	-60	-5	-5	10.16	0.45
Pales 1-605 model 26	-60	-5	0	7.11	0.47
Pales 1-605 model 27	-60	-5	5	7.12	0.44

The PALES program was developed by (5).

a) Displacements, in Å, of the coordinate center of the SBD from the center of the NBD.

Note: x and y axes are interchanged in the PALES output.

b) Sum of Euler angles in the z,y,z convention

c) $\eta = \left(S_{xx} - S_{yy}\right) / S_{zz}$

d) experimental values for the NBD of Hsc70 in PEG/hexanol (6) and the NBD of DnaKTTH in Pf1 phage (Zuiderweg, unpublished).

Supplementary Table 5: Raw NH RDC data for DnaK(1-605)														
Resnr	AA	RDC		Resnr	AA	RDC		Resnr	AA	RDC		Resnr	AA	RDC
4	I	-1.4		150	Q	17.8		322	V	-3.1		479	D	21.1
6	G	17.5		154	T	9.6		324	L	15.2		480	A	8.1
7	I	64.4		156	D	38.6		326	D	-1.5		482	G	20.1
8	D	4.2		157	A	18.5		329	L	-5.2		484	L	18.9
9	L	-21.7		158	G	18.3		330	S	-14.7		485	H	17.8
17	A	13.9		161	A	5.5		331	V	-11.2		486	V	20.2
18	I	-2.9		162	G	25.9		334	I	-12.9		487	S	17.8
20	D	-1.6		164	E	14.8		335	D	-5.5		488	A	13.7
21	G	10.6		165	V	10.4		336	D	5.0		489	K	15.1
27	L	16.8		167	R	-7.8		338	I	19.7		490	D	8.9
28	E	-1.6		168	I	-8.6		339	L	12.5		491	K	5.7
29	N	-8.5		177	L	17.7		341	G	-46.3		492	N	12.7
31	E	15.1		181	L	1.0		349	V	-6.1		493	S	13.1
32	G	-13.8		183	K	-15.1		350	Q	-9.2		494	G	8.9
35	T	-9.7		185	T	-1.9		358	G	17.5		496	E	3.1
39	I	20.4		186	G	-9.5		359	K	-2.4		497	Q	13.6
40	I	7.0		189	T	14.4		360	E	1.6		499	I	18.3
41	A	10.9		190	I	-6.8		362	R	9.4		503	A	1.2
45	D	5.7		192	V	-19.5		363	K	12.2		504	S	8.5
46	G	1.9		193	Y	14.2		365	V	18.7		505	S	3.7
47	E	-25.5		207	I	-2.3		379	G	-25.7		506	G	-10.8
48	T	-1.0		208	D	8.4		380	G	-7.7		523	A	-22.8
51	G	21.1		214	K	12.9		399	L	17.9		524	E	-5.1
52	Q	-1.6		215	T	9.2		400	G	23.0		554	G	-15.0
54	A	-7.0		217	E	7.8		401	I	15.2		555	D	8.7
55	K	-65.1		218	V	2.8		403	T	8.1		557	L	11.0
56	R	-7.0		219	L	9.6		404	M	10.0		559	A	-17.6
60	T	-13.7		220	A	8.6		405	G	18.4		560	D	-13.8
61	N	8.5		221	T	-43.1		406	G	13.8		561	D	-8.2
63	Q	-7.3		223	G	8.8		407	V	-4.5		564	A	-10.8
64	N	-13.0		224	D	17.8		409	T	15.1		568	A	-11.9
66	L	1.4		225	T	23.7		410	T	6.0		569	L	-16.1
67	F	9.3		226	H	7.6		411	L	26.9		570	T	-28.5
68	A	8.7		227	L	-18.8		413	A	15.9		574	T	-54.7
74	G	10.6		228	G	-23.8		416	T	18.1		575	A	-12.6
75	R	22.9		233	D	-25.0		417	T	17.4		577	K	-23.1
77	F	2.3		236	L	-10.7		420	T	20.5		578	G	0.6
78	Q	-13.7		237	I	-16.6		421	K	20.2		580	D	-6.1
79	D	7.3		248	Q	-15.5		423	S	10.9		583	A	-33.9
80	E	-2.1		249	G	8.4		425	V	18.4		584	I	-21.5
81	D	-21.7		250	I	6.2		429	A	-3.3		585	E	-49.9
82	V	22.6		253	R	-3.9		432	N	20.4		586	A	-2.8

83	Q	-27.9		254	N	-5.3		433	Q	-4.7		588	M	-16.3
87	S	44.5		255	D	8.3		436	V	-6.0		593	Q	-2.8
91	F	-1.3		257	L	-15.2		437	T	-6.0		594	V	-14.4
93	I	-14.0		258	A	4.8		438	I	12.2		596	Q	7.1
96	A	8.6		266	A	5.7		440	V	17.5		597	K	10.8
98	N	15.5		270	K	-8.9		441	L	15.8		598	L	-1.1
99	G	5.3		273	L	10.2		444	E	4.7		599	M	5.7
102	W	6.0		278	Q	-4.7		448	A	-24.2		602	A	2.8
103	V	-15.4		279	T	3.9		449	A	-24.8		603	Q	2.2
105	V	-10.8		281	V	-9.2		450	D	14.3				
106	K	-12.0		287	T	12.8		451	N	-12.5				
107	G	1.6		291	T	6.0		455	G	-1.6				
108	Q	8.4		292	G	14.2		456	Q	9.9				
109	K	-1.9		295	H	-15.8		457	F	11.6				
110	M	-12.7		296	M	-15.1		458	N	8.0				
111	A	-1.0		297	N	-7.5		459	L	-4.9				
118	E	12.5		298	I	-12.8		460	D	-16.7				
119	V	23.5		299	K	-20.7		461	G	5.3				
129	D	55.8		300	V	3.4		463	N	-1.4				
131	L	-64.5		301	T	-1.1		465	A	4.1				
132	G	-13.1		302	R	11.9		468	G	8.2				
135	V	-14.0		309	V	13.2		471	Q	9.2				
136	T	-4.6		310	E	-16.8		472	I	3.1				
137	E	11.3		311	D	-7.6		473	E	11.0				
140	I	-1.0		312	L	-3.9		474	V	12.3				
141	T	-51.1		315	R	-15.1		476	F	20.8				
146	F	19.9		317	I	-22.5		477	D	21.2				
148	D	21.7		318	E	-15.7		478	I	20.6				

Supplementary Table 6: Raw NH RDC data for DnaK(1-638)														
Resnr	AA	RDC		Resnr	AA	RDC		Resnr	AA	RDC		Resnr	AA	RDC
4	I	4.0		157	A	20.3		302	R	21.1		473	E	15.0
6	G	18.5		158	G	-3.0		310	E	-35.6		474	V	15.7
7	I	3.9		161	A	10.7		311	D	-5.7		476	F	21.1
18	I	0.8		162	G	12.6		329	L	-12.4		477	D	31.1
20	D	-4.2		164	E	18.1		330	S	-29.4		478	I	25.6
21	G	11.4		165	V	15.0		331	V	-8.9		479	D	14.3
27	L	9.9		167	R	-1.8		334	I	-5.9		480	A	2.2
28	E	6.8		170	N	-6.5		336	D	11.4		485	H	28.0
29	N	-7.9		177	L	28.4		338	I	27.4		486	V	42.2
31	E	-4.9		181	L	2.1		349	V	2.7		488	A	24.3
35	T	2.2		183	K	-28.1		360	E	2.6		489	K	21.2
40	I	19.4		185	T	-0.7		362	R	11.4		490	D	10.9
41	A	21.3		186	G	-9.6		363	K	9.8		491	K	9.2
45	D	4.9		190	I	14.9		379	G	-14.5		493	S	-5.3
46	G	-1.3		192	V	-29.3		380	G	-0.4		496	E	10.6
47	E	-19.0		193	Y	8.4		382	L	-25.2		497	Q	25.5
48	T	0.4		207	I	-5.7		383	T	3.3		499	I	23.9
51	G	13.7		210	V	11.5		384	G	3.1		504	S	8.6
52	Q	-11.7		211	D	16.8		387	K	9.1		505	S	4.3
54	A	-18.7		212	G	6.1		388	D	4.6		506	G	-12.3
56	R	-12.8		213	E	14.7		390	L	8.2		524	E	-1.4
60	T	8.7		214	K	16.3		393	D	12.7		554	G	-21.9
61	N	9.4		215	T	11.9		394	V	-1.1		555	D	13.3
63	Q	1.2		217	E	27.5		395	T	11.1		557	L	17.1
66	L	14.5		218	V	2.8		399	L	24.4		559	A	-15.6
67	F	7.6		225	T	8.7		400	G	26.6		564	A	-11.9
74	G	10.0		227	L	-25.6		401	I	0.3		578	G	-9.1
75	R	6.8		241	V	0.5		403	T	13.5		580	D	-3.5
77	F	-1.6		247	D	-12.8		409	T	31.2		593	Q	-10.9
78	Q	-5.0		249	G	4.8		410	T	13.7		638	K	1.1
79	D	10.5		250	I	6.7		413	A	16.5				
80	E	10.2		253	R	-1.6		417	T	16.7				
91	F	-4.4		254	N	-6.4		420	T	33.2				
96	A	4.9		255	D	13.5		421	K	29.5				
98	N	9.9		257	L	3.9		423	S	17.2				
99	G	6.0		266	A	13.4		437	T	9.7				
105	V	-14.3		268	K	2.7		438	I	14.2				
106	K	-8.4		270	K	-12.8		439	H	13.7				
107	G	2.1		273	L	9.8		440	V	29.5				
108	Q	17.4		278	Q	3.9		441	L	18.6				
109	K	2.1		279	T	4.7		455	G	-0.5				
110	M	-22.6		281	V	-11.4		456	Q	19.7				

111	A	-1.2		287	T	5.7		457	F	8.0				
118	E	22.9		291	T	2.5		458	N	8.8				
132	G	-10.4		292	G	18.8		459	L	-5.9				
135	V	-14.5		295	H	-19.2		460	D	-16.5				
140	I	-6.1		297	N	-8.4		461	G	19.7				
141	T	14.1		298	I	-9.9		463	N	5.4				
146	F	13.6		299	K	-18.1		465	A	0.4				
148	D	14.5		300	V	7.2		471	Q	18.6				
150	Q	3.8		301	T	-1.3		472	I	16.4				

Supplementary Table 7. RDC selection procedure DnaK(1-605)						
Domain		Nr RDC's	Culled RDC's [a]	RMSD of fit (Hz)	Q of fit[b]	Θ(z) (Deg)
IA+IB+IIA		132		17.44	0.92	7.9
IA+IB+IIA		114	7,48,55,66,80,87,107,129, 131,140,141,156,181, 221,341,349,359	10.06	0.74	6.8
IA+IB+IIA		103	18,20,77,79,190,192,311,322,324,358,360	8.17	0.59	4.5
IA+IB+IIA		91	8,74,99,102,111,136,168,185,207,220,228,326	7.63	0.53	-4.3
IIB		31		8.47	0.68	15.7
IIB		25	228,233,253,270,300,301	5.32	0.49	13.3
IIB		22	266,287,291	4.41	0.36	14.9
Beta+LID		99		9.53	0.59	-5.82
Beta+LID		83	429,433,444,461,463,465,468,472,503,505,506, 578,598,602	7.48	0.44	-5.11
Beta+LID		77	411,457,458,524,564,586	6.59	0.38	-2.4

a) RDC's were iteratively culled according to the following two rules :

when $|(RDC_{exp}-RDC_{comp})/RDC_{exp}| > 2Q$

when $| RDC_{exp} | > 3|D_a|$

b) $Q = RMSD / \sqrt{\sum RDC_{\exp}^2}$

Supplementary Table 8. RDC selection procedure DnaK(1-638)						
Domain		Nr RDC's	Culled RDC's [a]	RMSD of fit (Hz)	Q of fit[b]	Θ(z) (deg)
IA+IB+IIA+IIB		119		10.8	0.83	6.45
IA+IB+IIA+IIB		97	18,31,35,46,48,63,79,80,158,167,181, 185,210,241,253,257,268,301,311,360, 380,383,384	10.27	0.71	0.41
IA+IB+IIA+IIB		86	7,60,75,99,107,207,211,250,334,349,380	9.63	0.64	-2.4
IA+IB+IIA+IIB		78	77,111,141,192,249,270,291,297	7.87	0.52	-4.0
IA+IB+IIA+IIB		72	45,105,109,193,218,227	6.92	0.45	-7.2
Beta+LID		54		10.10	0.57	-10.95
Beta+LID		45	401,437,455,461,465,480,506,524,578	7.02	0.36	-8.3
Beta+LID		42	471,472, 564	5.84	0.30	-4.8

a) RDC's were iteratively culled according to the following two rules :

when $|(RDC_{exp}-RDC_{comp})/RDC_{exp}| > 2Q$

when $| RDC_{exp} | > 3|D_a|$

b) $Q = RMSD / \sqrt{\sum RDC_{\exp}^2}$

References.

1. Zhu G, Xia Y, Nicholson LK, & Sze KH (2000) Protein dynamics measurements by TROSY-based NMR experiments. *J. Magn. Reson.* 143(2):423-426.
2. Woessner DE (1962) Nuclear Spin Relaxation in Ellipsoids Undergoing Rotational Brownian Motion. *J. Chem. Phys.* 37(3):647-654.
3. Lipari G & Szabo A (1982) Model-Free Approach to the Interpretation of Nuclear Magnetic-Resonance Relaxation in Macromolecules. 1. Theory and Range of Validity. *J. Am. Chem. Soc.* 104(17):4546-4559.
4. Chang L*, et al.* (2008) High-throughput screen for small molecules that modulate the ATPase activity of the molecular chaperone DnaK. *Anal Biochem* 372(2):167-176.
5. Zweckstetter M & Bax A (2001) Characterization of molecular alignment in aqueous suspensions of Pf1 bacteriophage. *J Biomol NMR* 20(4):365-377.
6. Zhang Y & Zuiderweg ER (2004) The 70-kDa heat shock protein chaperone nucleotide-binding domain in solution unveiled as a molecular machine that can reorient its functional subdomains. *Proc Natl Acad Sci U S A* 101(28):10272-10277.